NETWORKS AND HETEROGENEOUS MEDIA
©American Institute of Mathematical Sciences
Volume **1**, Number **4**, December **2006**

Website: http://aimSciences.org

pp. **621–637**

# EXOGENOUS CONTROL OF VASCULAR NETWORK FORMATION IN VITRO: A MATHEMATICAL MODEL

V. Lanza, D. Ambrosi and L. Preziosi

Dipartimento di Matematica
Politecnico di Torino
Corso Duca degli Abruzzi, 24, Torino, 10123, Italy

Abstract. The reconstitution of a proper and functional vascular network is a major issue in tissue engineering and regeneration. The limited success of current technologies may be related to the difficulties to build a vascular tree with correct geometric ratios for nutrient delivery. The present paper develops a mathematical model suggesting how an anisotropic vascular network can be built *in vitro* by using exogenous chemoattractant and chemorepellent. The formation of the network is strongly related to the nonlinear characteristics of the model.

1. **Introduction.** Tissue engineering and regeneration is considered one of the hottest medical frontiers of the new millennium. However a relevant difficulty, which hampers the current efforts to gain robust results, is to provide bulk tissues with a vascular network characterized by an architecture suitable for delivering nutrients and eliminating wastes [20]. Actually, to achieve these results, vertebrates have evolved a hierarchical branching blood vascular system that terminates in a network of size-invariant units, namely capillaries. The capillary networks are characterized by typical intercapillary distances ranging from 50 to 300 $\mu$m which is instrumental for optimal metabolic exchange [11, 17, 3]. Depending on the tissue, *in vivo* vasculature can show no preferential direction and therefore a substantial isotropy, as in the liver, or a strong anisotropic structure, as in the skin. The anisotropy is either related to the non isotropic characteristics of the substratum or controlled by the presence of chemoattractants, e.g. Vascular Endothelial Growth Factor-A (VEGF), and chemorepellents, e.g. semaphorines, which are well known to drive the path of the axons [10]. It is therefore important to understand how to reproduce such characteristics *in vivo*.

As reviewed in [1], an approach to build small-diameter vessels *in vitro* is to use endothelial cells (EC), smooth muscle cells or endothelial progenitors seeded on scaffolds based on either a biodegradable or decellularized matrix [12, 13, 20, 25]. In fact, single randomly dispersed endothelial cells self-organize to form networks like those shown in Figure 1. After 12–16 hours the geometric tubular network eventually formed is very similar to isotropic vascular beds produced *in vivo* by

2000 *Mathematics Subject Classification.* Primary: 92C15, 92C17; Secondary: 92C50.

*Key words and phrases.* Mathematical Modelling, Pattern Formation, Vascularization, Tissue Engineering.

The work has been partially funded by the MC-RTN Project MRTN-CT-2004-503661 "Modelling, mathematical methods and computer simulation for tumour growth and therapy" and by the FIRB project RBAU01K7M2 "Metodi dell'analisi matematica in biologia, medicina e ambiente".

vasculogenesis [18, 9]. This phenomenon has been called *in vitro* angiogenesis [6]. A partial movie of an experiment can be viewed at the EMBO web site as supplementary material to the paper by Serini et al. [22].

Gamba *et al.* [8], Serini *et al.* [22] and Ambrosi *et al.* [2] worked on a mathematical model based on the main hypothesis that endogenous chemotaxis and persistence in cell motion are the key mechanisms in the initial stages of the process. The model is able to reproduce the formation of capillary networks *in vitro* starting from a moderate number of cells. They related the characteristic size of the network with the range of activity of a specific chemoattractant (Vascular Endothelial Growth Factor-A) acting by autocrine/paracrine mechanisms (more precisely, the typical cord length is the square root of the product of the diffusion coefficient and the half life of vascular endothelial growth factor-A, in good agreement with phenomenological observations *in vivo* and measurements *in vitro*).

The model also reproduced the experimental observation that a strictly constrained density of endothelial cells (ranging from 100 to 400 cells/mm$^2$) is a critical parameter allowing the formation of a capillary network with an architecture similar to that found *in vitro*. In fact, below such a range groups of disconnected structures form. Coniglio et al. [4] studied this abrupt transition showing that it is a percolative transition. Above such a range thicker chords of the same lenght form. Eventually, for very high cell densities the experiments give rise to the formation of a continuous carpet of cells with holes or lacunae. This transition was studied by Kowalczyk et al. [16] who focused on the stability of the uniform solution (the "continuous carpet").

Filbet et al. [5] and Merks et al. [19] studied the same problem using different modeling approaches, namely kinetic models and Potts models, respectively. In particular, Filbet et al. [5] derived the model using a Chapman-Eskog expansion of a kinetic velocity-jump process. The individual based model used in [19] allowed instead to consider sub-cellular phenomena such as adhesion and receptor dynamics.

Recently, Tosin et al. [24] modified the original model including the mechanical interaction between the cells and the substratum thanks adhesion forces. The reader is referred to the review article [1] for more details on the relevant experimental details and on the related mathematical models.

In this paper, we generalize the model in [8, 22, 2] to include anisotropic effects induced by exogenous chemoattractants and chemorepellents in view of the simulation of experimental set-ups aimed at the formation of anisotropic vascular networks controlled from the outside. It is in fact thought that the application of this model to tissue engineering may be helpful in designing devices to generate a functional vascular bed in synthetic or decellularized natural matrix scaffolds. Actually, the use of scaffolds containing different combinations of angiogenic inducers has been demonstrated to be promising in the establishment of a mature vasculature in ischemic tissue [21]. Here it is found that a key role is played by the nonlinear term describing cell persistence and by the range of action of the chemical factors. Chemoattractants promote the formation of capillaries which depart from the source of chemoattractants. On the contrary, chemorepellents induce the formation of capillaries which tend to run around the source of chemorepellent, where the range of influence is fading away. Outside the range of influence of the exogenous chemical factors, the capillaries connect to a more or less isotropic network which forms spontaneously under the action of endogenous chemoattractants.

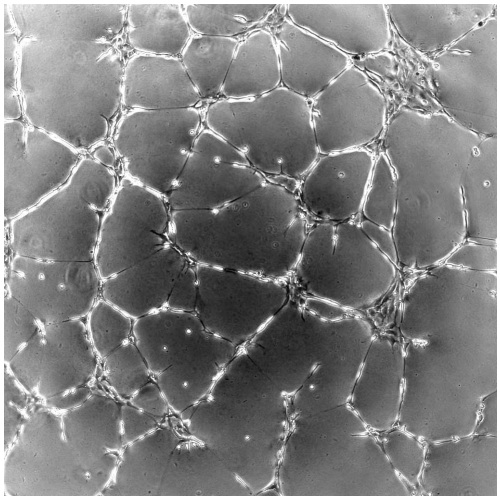

FIGURE 1. Vascular network on a Matrigel surface. The box-side is 2 mm.

The paper develops as follows. Section 1 is devoted to the deduction of the model. In Section 2 are described the effects of exogenous chemoattractans, e.g. VEGF, while the role of exogenous chemorepellents, e.g. semaphorines, is discussed in Section 3. Finally, Section 4 gives some analytical results on the boundness and positivity of the solution.

2. **The mathematical model.** In recent years Gamba et al. [8], Serini et al. [22] and Ambrosi et al. [2] have proposed a mathematical model able to describe vascular network formation assuming that persistence and chemotaxis are the key features determining the pattern. Their model predicts the formation of isotropic structures.

Having in mind possible applications to tissue engineering, here we focus on the external control of the characteristics of the network through the use of exogenous chemical factors. From the experimental viewpoint this can be achieved adding to the substratum gelly sponges or "spaghetti–shape" sources of chemical substances able to attract or repel endothelial cells (e.g., VEGF and semaphorines, respectively).

The model proposed in the literature mentioned above can then be modified as follows

$$\frac{\partial n}{\partial t} + \nabla \cdot (n\mathbf{v}) = 0\,, \tag{1}$$

$$\frac{\partial \mathbf{v}}{\partial t} + \mathbf{v} \cdot \nabla \mathbf{v} = \beta \nabla c + \beta_a \nabla c_a - \beta_r \nabla c_r - \gamma \mathbf{v} - \nabla \varphi(n)\,, \tag{2}$$

$$\frac{\partial c}{\partial t} = D\Delta c - \frac{c}{\tau} + \alpha n\,, \tag{3}$$

$$\frac{\partial c_a}{\partial t} = D_a \Delta c_a - \frac{c_a}{\tau_a} + s_a(t) H_a(\mathbf{x})\,, \tag{4}$$

$$\frac{\partial c_r}{\partial t} = D_r \Delta c_r - \frac{c_r}{\tau_r} + s_r(t) H_r(\mathbf{x})\,, \tag{5}$$

where $n(\mathbf{x},t)$ and $\mathbf{v}(\mathbf{x},t)$ are the density and velocity of the endothelial cells (EC), respectively, $c(\mathbf{x},t)$ is the concentration of vascular endothelial growth factor (VEGF-A) produced by endothelial cells (hereafter denoted as endogenous chemoattractant), $c_a(\mathbf{x},t)$ is the concentration of exogenous chemoattractant, and $c_r(\mathbf{x},t)$ is the density of exogenous chemorepellent. The chemotactic forces may include a saturation term $\beta/(1+c/c_M)$, $\beta_i/(1+c_i/c_{iM})$, $i=a,r$.

Equation (1) is a mass conservation equation for the cell matter, corresponding to the observation that cells do not undergo mitosis or apoptosis on the patterning time scale. Equations (3)-(5) are diffusion equations for the chemical factors involved. According to (3) the endogenous chemoattractant is produced by the endothelial cells at rate $\alpha$ and degrades with half life $\tau$. In (4) and (5) the chemical factors are released at a rate $s_a(t)$ and $s_r(t)$ in some domains identified by the indicator functions $H_a$ and $H_r$, which vanish outside the domain where the exogenous chemical factor has a constant concentration equal to 1.

Although Eq.(2) is reminiscent of the momentum balance equation for the cellular matter, the nonlinear term does not actually account for inertia, but it rather models the delayed response of the cell due to the time needed to re-organize the internal cytoskeleton to change the direction of motion. Therefore cells do not immediately detect and respond to chemotactic signals by modifying in real time their trajectory but show what biologists call *persistence* in keeping their direction [27, 28, 7] or, in physical terms, an "inertia" in changing cell direction. Neglecting the nonlinear convective term on the left hand side would lead to cell clustering around the points of maximum concentration of chemoattractant, as in many classical chemotactic models. Instead, by a non linear dynamical mechanism similar to that encountered in fluid dynamics, this term is responsible for the formation of shock-like structures: cells climb along the saddle lines of the concentration field thus forming chords, eventually producing a network structure.

It is an intriguing paradox that the behavior of living matter as cells is so well reproduced by equations that are deduced for inert matter (*inertia* in Latin means "without ability"). However it is not a surprise that nonlinear convective terms are able to generate patterns: when removing the right hand side in equation (2) one gets the multidimensional inviscid Burgers equation. Burgers equation is a well established paradigm in the theory of self-organized aggregation and pattern formation, which has been utilized to describe the emergency of structured patterns in many different settings (see, for instance, [23, 26]). The present setting is rather different because trajectories are here essentially dictated by the chemical field and not by the initial velocities. However the mechanism of placement of matter between nodes, that is the tendency to preserve the trajectory (or momentum conservation) is analogous.

The right hand side of the persistence equation (2) should then be understood as a phenomenological way to describe the drivers of the direction of motion. They are (from right to left) the pressure force inhibiting cell overcrowding, the drag force between cells and the substratum, and, most important, the chemotactic forces. The positive and negative sign of the chemotactic action accounts for attraction or repulsion, respectively. Regarding the pressure term, we will assume the following characterization: it vanishes below a density $n_0$ corresponding to the beginning of cell confluence and is a convex function for larger $n$.

It can be noticed that if VEGF-A itself is used as an exogenous chemoattractant then Eq.(4) can be merged into Eq.(3) giving

$$\frac{\partial c}{\partial t} = D\Delta c - \frac{c}{\tau} + \alpha n + s(t)H_a(\mathbf{x})\,, \tag{6}$$

with only one chemotactic term $\beta\nabla c$ in Eq.(2).

As diffusion is a much faster process than cell aggregation, the time derivative in the diffusion equations can be dropped. Scaling distances with the size $L$ of the visual field, times with $\sqrt{D/\alpha\beta n_0}$, the density with the cell density at confluency $n_0$, concentration of endogenous chemical factor with $\alpha n_0 L^2/D$ and of exogenous chemical factors with $s_i L^2/D_i$, $(i = a, r$, if $s_i$ is constant), the system of equations (1)-(5) can be written in dimensionless form as

$$\begin{aligned}
\frac{\partial n^*}{\partial t^*} + \nabla\cdot(n^*\mathbf{v}^*) &= 0\,, &(7)\\
\frac{\partial \mathbf{v}^*}{\partial t^*} + \mathbf{v}^*\cdot\nabla\mathbf{v}^* &= \nabla c^* + \beta_a^*\nabla c_a^* - \beta_r^*\nabla c_r^* - \gamma^*\mathbf{v}^* - \nabla\varphi^*(n^*)\,, &(8)\\
\Delta c^* - \frac{c^*}{\xi^2} + n^* &= 0\,, &(9)\\
\Delta c_a^* - \frac{c_a^*}{\xi_a^2} + H_a(\mathbf{x}^*) &= 0\,, &(10)\\
\Delta c_r^* - \frac{c_r^*}{\xi_r^2} + H_r(\mathbf{x}^*) &= 0\,, &(11)
\end{aligned}$$

where

$$\xi = \frac{\sqrt{D\tau}}{L}\,, \qquad \gamma^* = \gamma\sqrt{\frac{D}{\alpha\beta n_0}}\,, \qquad \varphi^*(n^*) = \frac{D}{\alpha\beta n_0 L^2}\varphi(n_0 n^*)\,,$$

$$\xi_i = \frac{\sqrt{D_i\tau_i}}{L}\,, \qquad \beta_i^* = \frac{\frac{\beta_i s_i}{D_i}}{\frac{\beta\alpha n_0}{D}}\,, \qquad i = a, r\,.$$

The equations will be solved starting from the following initial conditions

$$\begin{cases} n^*(\mathbf{x}^*,\, t^*=0) &= \dfrac{1}{2\pi r^2}\displaystyle\sum_{j=1}^{M}\exp\left(-\frac{\left|\,\mathbf{x}^* - \mathbf{x}_j^*(\omega)\right|^2}{2r^2}\right)\\[2ex] \mathbf{v}(\mathbf{x}^*,\, t^*=0) &= 0, \end{cases}$$

where $r$ is the dimensionless radius of a cell. The initial conditions above simulate the experimental ones where cells are random dispersed on the Matrigel, a surface which favors cell motility and has biochemical characteristics similar to living tissues. In addition, unless when differently specified, periodic boundary conditions are used.

It is known [8, 22, 2] that the diffusion equation (9) introduces a characteristic length $\ell = \sqrt{D\tau}$ determining the size of the chords in the network structure in absence of other external influences. We will see that in a similar way the other two diffusion equations (4) and (5) are characterized by the natural lengths $\ell_a = \sqrt{D_a\tau_a}$ and $\ell_r = \sqrt{D_r\tau_r}$, related to the range of action of the chemoattractant and chemorepellent, respectively. In the next section it is shown that cells located at a distance smaller than these ranges, are strongly influenced by the exogenous chemical factors; at longer distance endogenous chemotaxis governs the formation of a more isotropic network.

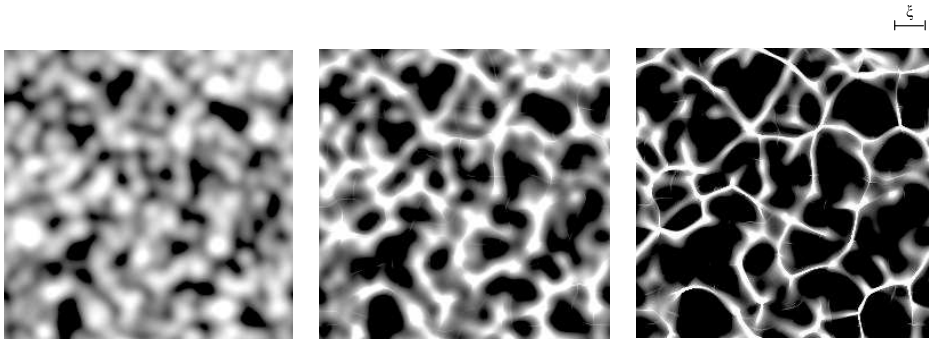


FIGURE 2. Formation of the network structure without any exogenous action. The result can be compared with Figure 1. The bar indicates the value of $\xi = 0.1$, i.e. the order of magnitude of the range of action of VEGF, the endogenous chemoattractant.

3. **The effect of exogenous chemoattractant.** The system of equations (7)-(11) has been discretized on the unit square using $2^n$ equispaced nodes with periodic boundary conditions. A finite volume numerical scheme of Godunov type has been adopted for the hyperbolic part in Equations (7) and (8) (*i.e.*, transport and pressure) and a simple centered discretization has been used for the chemotactic term. Equations (9)–(11) have been discretized by a spectral approach and solved by Fast Fourier Transform.

Figure 2 reports the result of a numerical simulation in absence of any exogenous action. The value of $\gamma^*$ used in this and all the results that follow is equal to 1. The results well compare with the experiments shown in Fig. 1 as quantitatively described in [22].

In all simulations a density field corresponding to 800 cells seeded is initially set up, with a cell radius of 45 $\mu$m, on a 2 mm$\times$ 2 mm square. The initial cell density is therefore equal to 200 cells/mm$^2$, above the critical density $n_c \approx 100$ cells/mm$^2$ that gives rise to the percolative transition studied in [4]. The experimentally measured value of the diffusion coefficients and the decay time were $D \approx 10^{-7}$ cm$^2$/s and $\tau = 3840$ s, so that the dimensionless distance is

$$\xi = \frac{\sqrt{10^{-7}\mathrm{cm}^2/\mathrm{s} \cdot 3840\mathrm{s}}}{0.2\mathrm{cm}} = 0.0978\,\mathrm{cm},$$

respectively (see [22]). In absence of experimental evidence the chemotactic parameters are set $\beta_a^* = \beta_r^* = 1$.

As a first example of external action we consider the case in which the source of exogenous chemoattractant is located on the boundary on two opposite sides of the domain, experimental setting which can be obtained putting some sponges impregnated with chemoattractant on the border of the Petri-dish. In this case Eq.(10) slightly modifies since there is no source term and the concentration of chemoattractant in the sponges (assumed constant in time) rewrites in the boundary conditions

$$c_a(x = 0, y, t) = c_a(x = L, y, t) = \tilde{c}_b\,, \qquad \forall\, y \in [0, L]\,, \tag{12}$$

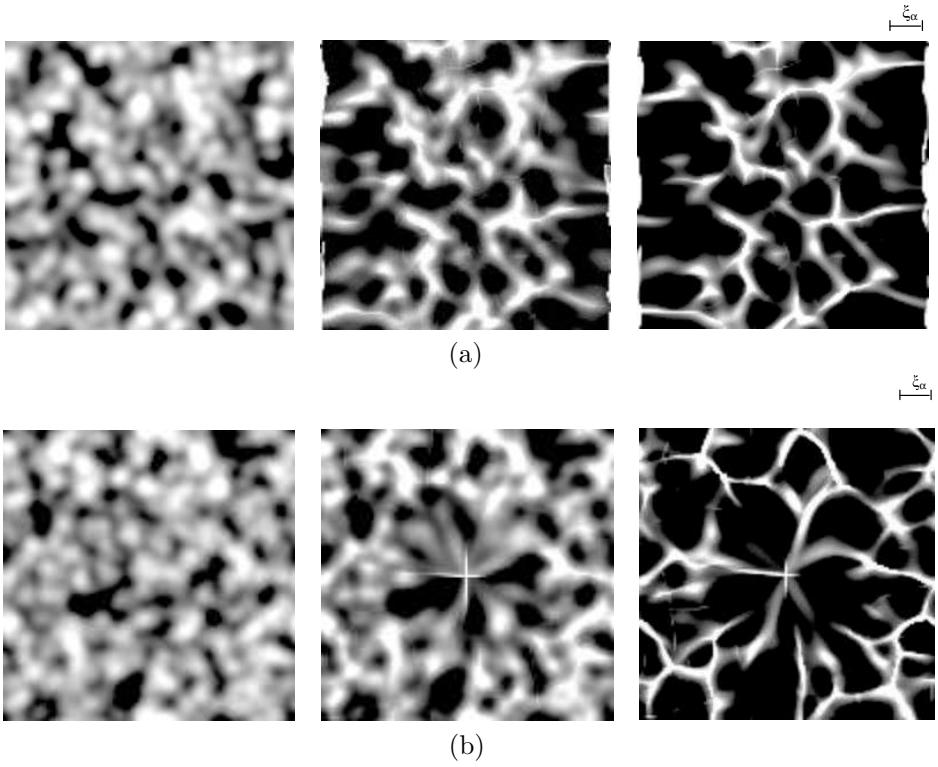


FIGURE 3. Network formation influenced by an exogenous chemoattractant. In (a) the chemical factor is placed on the right and on the left of the domain, and in (b) it is placed in the center of the domain. Bars indicate the value of $\xi_a = 0.1$, i.e. the order of magnitude of the range of action of the exogenous chemoattractant.

together with periodic boundary conditions on the remaining sides $y = 0, L$. Actually, in this simple geometry Eq.(10) can be readily solved so that the concentration

$$c_a = \tilde{c}_b \frac{e^{x/\ell_a} + e^{(L-x)/\ell_a}}{1 + e^{L/\ell_a}},$$

can be directly substituted in (8).

In the simulation presented in Figure 3a the exogenous and endogenous chemoattractant were the same, so that $\ell_a = \ell$. Figure 3a then shows that in a range $\ell$ from the sides $x = 0$ and $x = L$ capillaries organize themselves perpendicularly to the sides. At a distance of order $\ell$ they branch off giving rise to a capillary network very similar to the one obtained in the isotropic case.

In Figure 3b the chemoattractant is placed in the center of the domain, i.e. $H_a(\mathbf{x}) = \delta(\mathbf{x} - \mathbf{x}_0)$. This source placement gives rise to a circular zone influenced by the chemical factors characterized by the formation of capillaries arranged in radial direction.

4. **The effect of exogenous chemorepellent.** The use of chemorepellent factors originates the patterns shown in Fig. 4. In particular, the chemorepellent factor is placed in the center of the domain. Cells then move away from the central region

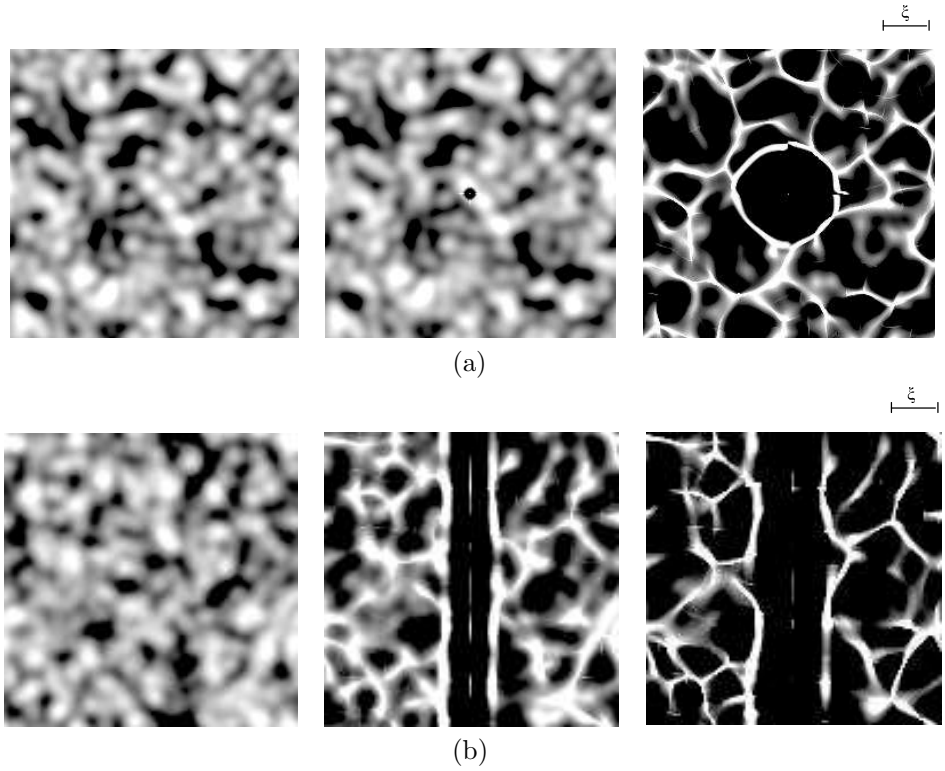


FIGURE 4. Network formation influenced by an exogenous chemorepellent. In (a) the chemical factor is placed in the center, while in (b) it is placed on the central axis of the domain. Bars indicate the value of $\xi_r = 0.158$, i.e. the order of magnitude of the range of action of the exogenous chemorepellent.

(moving more or less radially) accumulating in a growing circumference with faster cells catching up slower ones according to the nonlinear dynamics explained in Section 2. In fact, cells nearer the center move faster.

A circular capillary loop forms, connected with the more isotropic external structure. The final size of the circular capillary loop corresponds to the range of action of the chemorepellent. In fact, in the simulation the values of the parameters give $\ell_r = 0.31$ mm, which in dimensionless form corresponds to the theoretical value $\xi_r = 0.158$. This value closely corresponds to that in Figure 4a.

In a second simulation (Figure 4b) the chemorepellent source is placed along a line parallel to the $y$-axis. Also in this case cells move away from the central axis, along $x$ accumulating along two lines parallel to the $y$-axis at a distance close to the range of the chemorepellent. This way a capillary parallel to the stripe of chemorepellent is formed and connects with the outer network structure.

As in the previous example, the distance between the two capillaries which run parallel to the stripe of chemorepellent is nearly twice the range of action of the chemorepellent (0.27 compared with the theoretical value 0.316).

The mechanisms illustrated above can be used to design a vascular network. For instance, assuming that we want to reproduce a network structure characterized by

FIGURE 5. Results of the simulation in presence of three stripes of chemorepellent placed at a reciprocal distance $d = \frac{L}{4}$. The length of the stripes is $\frac{L}{2}$.

a region where capillaries run in parallel at a distance $d$ (as it occurs, for instance, in the skin) one can theoretically use, if possible, chemorepellents characterized by a range of action of the order of $d/2$ and place the stripes at a distance $\approx d$. Figure 5 shows the final result obtained using this virtual distribution. In fact, in this case cells are repelled from the stripes moving perpendicularly to the stripes. They align in the middle of the stripe forming the capillaries.

Similarly to what happens in the other cases shown in Figure 4, outside the region influenced by the chemorepellent, the capillary coalesce and connect to the external network.

5. **Blow-up control by the pressure term.** In this section it is discussed how the pressure term $\varphi(n)$ affects the boundness of the solution, following the approach in [14]. We concentrate on the case in which only an exogenous chemorepellent is present, because considering the exogenous chemoattractant only involves a non essential extra term in the model and the generalization of the theorems below is trivial.

As in [14], we neglect the effect of persistence and consider the following problem

$$\begin{cases} \dfrac{\partial n}{\partial t} = \nabla \cdot (f(n)\nabla n - \chi n \nabla c + \chi_r n \nabla c_r)\,, \\ \Delta c - \mu c + a n = 0\,, \\ \Delta c_r - \mu_r c_r + \frac{H_r(\mathbf{x})}{D_r} = 0\,, \\ \nabla n \cdot \mathbf{N} = \nabla c \cdot \mathbf{N} = \nabla c_r \cdot \mathbf{N} = 0 \qquad \text{in} \quad [0, T_{max}) \times \partial\Omega\,, \\ n(0, \mathbf{x}) = n_0(\mathbf{x}) \qquad \text{in} \quad \Omega\,, \end{cases} \tag{13}$$

where $f(n) = \frac{n}{\gamma}\varphi'(n)$, $a = \frac{\alpha}{D}$, $\mu = (\tau D)^{-1}$, $\mu_r = (\tau_r D_r)^{-1}$, $\chi = \frac{\beta}{\gamma}$, $\chi_r = \frac{\beta_r}{\gamma}$. In addition, $T_{max}$ is such that, for every $t \in (0, T_{max})$ the solution $n(t, \mathbf{x})$ belongs to the space $L^\infty(\Omega) \cap H^1(\Omega)$ with $\frac{\partial n}{\partial t} \in L^1(\Omega)$. The function $n_0$ is a nonnegative function depending on $\mathbf{x}$, such that $n_0(\mathbf{x}) \in L^\infty(\Omega)$, where $\Omega$ is a domain with a

$C^{1,1}$ boundary*. We assume here that the Lebesgue measure of $\Omega$, $|\Omega|$, is equal to 1, without loss of generality. The vector $\mathbf{N}$ finally denotes the outward normal to the boundary $\partial\Omega$.

It can be noticed that the equation for the chemorepellent is independent from the others, so it will be useful to recall that, for instance, since $H_r(\mathbf{x}) \in L^p$, $c_r \in W^{2,\infty}(\Omega) \cap H^3(\Omega) = \{v \in L^\infty(\Omega) | D^\alpha v \in L^\infty(\Omega), D^\beta v \in L^2(\Omega), \forall\, \alpha \in \mathbb{N}^d, |\alpha| \leq 2, \forall\, \beta \in \mathbb{N}^d, |\beta| = 3\}$.

Notice that neglecting the persistence term, we obtain an aggregation model very close to the Keller-Siegel one with nonlinear diffusion. In particular, its possibility of blow up of solutions in a finite time and local existence of solutions have been studied in great detail in the literature.

To prove the nonnegativity of the solution we use the same technique used in [14] and consider the following auxiliary problem:

$$\begin{cases} \dfrac{\partial n}{\partial t} = \nabla \cdot (\tilde{n}(h'(n)\nabla n - \chi \nabla c + \chi_r \nabla c_r))\,, \\ \Delta c - \mu c + an = 0\,, \\ \Delta c_r - \mu_r c_r + \frac{H_r(\mathbf{x})}{D_r} = 0\,, \\ \nabla n \cdot \mathbf{N} = \nabla c \cdot \mathbf{N} = \nabla c_r \cdot \mathbf{N} = 0 \qquad \text{in} \quad [0, T_{max}) \times \partial\Omega\,, \\ n(0, \mathbf{x}) = n_0(\mathbf{x}) \qquad \text{in} \quad \Omega\,, \end{cases} \tag{14}$$

where $nh'(n) = f(n)$, $\tilde{n} = n^+$ and $n^+$ denotes the positive part of $n$. Multiply now the first equation in (14) by the negative part of $n$, $n^-$ and integrate over $\Omega$. Taking into account that $n = n^+ - n^-$, we obtain

$$\int_\Omega \frac{\partial n}{\partial t} n^- d\mathbf{x} - \frac{d}{dt}\left(\frac{1}{2}\int_\Omega (n^-)^2 d\mathbf{x}\right),$$

and

$$\begin{aligned} \int_\Omega n^- \nabla \cdot (\tilde{n}(h'(n)\nabla n - \chi \nabla c + \chi_r \nabla c_r)) d\mathbf{x} = \int_\Omega \tilde{n} h'(n) |\nabla n^-|^2 d\mathbf{x} \\ + \chi \int_\Omega \tilde{n} \nabla n^- \cdot \nabla c d\mathbf{x} - \chi_r \int_\Omega \tilde{n} \nabla n^- \cdot \nabla c_r d\mathbf{x}\,, \end{aligned} \tag{15}$$

where we used the no-flux boundary condition and the fact that $n^+ n^- = 0$. The three integrals on the right-hand side of (15) vanish because $\tilde{n} = n^+$, and so $\tilde{n}\nabla n^- = \mathbf{0}$ and $\tilde{n}|\nabla n^-|^2 = 0$. Thus we obtain

$$\int_\Omega (n^-)^2 d\mathbf{x} = \int_\Omega (n_0^-)^2 d\mathbf{x}\,, \tag{16}$$

where $n_0^-$ is the negative part of the function $n_0$. Since we have assumed that $n_0$ is nonnegative, the right-hand side of (16) vanishes. It follows that $n^- = 0$ a.e. and therefore $n$ is a nonnegative function. Since system (14) is equivalent to system (13), hence the solution of (13) is nonnegative too. The non-negativity of $c$ can be

*Here with $C^{1,1}$ we denote the vector space of the functions $\Omega \to \mathbb{R}$ that are $C^1$ and whose derivatives are Lipschitz-continuous.

proved as in [14] while the non-negativity of $c_r$ is well known and due to the fact that $H_r(\mathbf{x})$ is a source term.

In addition, it is important to notice that the model preserves mass, i.e. $||n(t)||_{L^1}$ is constant, provided that no-flux boundary conditions are imposed.

The following theorem will prove the boundness of the solution provided that the pressure term possesses physically sound properties, e.g. convexity.

**Theorem 1.** *Let $\Omega$ be an open, bounded domain in $\mathbb{R}^2$ with $C^{1,1}$ boundary. Assume that there exists $\bar{n} > 0$, such that*

$$f(n) \geq \frac{9\pi}{2} C_\Omega a \chi \theta + \delta \qquad \forall\, n \geq \bar{n}, \tag{17}$$

*for some arbitrarily small $\delta > 0$, $||n(t)||_{L^1} = 2\pi\theta \quad \forall\, t \in (0, T_{max})$ and $C_\Omega$ being a constant depending only on $\Omega$. Then for any finite $T \leq T_{max}$ the solution to the Problem* (13) *is uniformly bounded in* $[0, T]$.

*Proof.* The proof is based on the two following lemmas. □

**Lemma 1.** *Let $\Omega$ be an open, bounded domain in $\mathbb{R}^2$ with $C^{1,1}$ boundary. Assume that there exist $\varepsilon > 0$, $n_\varepsilon > 0$, such that $f(n) \geq 2\varepsilon$ for all $n \geq n_\varepsilon$. If*

$$\begin{aligned} &||\nabla c(t)||_{L^\infty} \leq C_1 \qquad \textit{for} \qquad 0 < t < T_{max}\,, \\ &||\nabla c_r||_{L^\infty} \leq C_2\,, \end{aligned} \tag{18}$$

*then*

$$||n(t)||_{L^\infty} \leq C_3 \max\{1, 2\pi\theta, ||n_0(t)||_{L^\infty}\} \qquad \textit{for} \qquad 0 < t < T_{max}\,,$$

*where $C_3$ depends on $C_1$ and $C_2$.*

*Proof.* The proof is similar to that in [14], except for the new terms that involve the chemorepellent concentration $c_r$. Take $p > 1$ and multiply the first equation in (13) by the $p$-th power of $n_m$, where

$$n_m = (n - m)^+$$

and $m$ is a positive constant to be found. Following [14] one can perform the following calculations

$$\begin{aligned} \int_\Omega \nabla \cdot (f(n)\nabla n - \chi n \nabla c + \chi_r n \nabla c_r) n_m^p \, d\mathbf{x} = \\ - \frac{4p}{(p+1)^2} \int_\Omega f(n) |\nabla n_m^{\frac{p+1}{2}}|^2 d\mathbf{x} + \chi p \int_\Omega (n_m^p + m n_m^{p-1}) \nabla c \cdot \nabla n_m d\mathbf{x} \\ - \chi_r p \int_\Omega (n_m^p + m n_m^{p-1}) \nabla c_r \cdot \nabla n_m d\mathbf{x}\,. \end{aligned} \tag{19}$$

The following upper bounds for the terms related with the endogenous chemoattractant can be proved

$$\chi p \int_\Omega n_m^p \nabla c \cdot \nabla n_m d\mathbf{x} \leq p \frac{\varepsilon}{(p+1)^2} \int_\Omega |\nabla n_m^{\frac{p+1}{2}}|^2 d\mathbf{x} + \frac{p\chi^2}{\varepsilon} C_1^2 \int_\Omega n_m^{p+1} d\mathbf{x}\,, \tag{20}$$

$$m\chi p\int_\Omega n_m^{p-1}\nabla c\cdot\nabla n_m d\mathbf{x}\le p\frac{\varepsilon}{(p+1)^2}\int_\Omega|\nabla n_m^{\frac{p+1}{2}}|^2 d\mathbf{x} + \frac{p(m\chi)^2}{\varepsilon}C_1^2\int_\Omega n_m^{p+1}d\mathbf{x}+\frac{p(m\chi)^2}{\varepsilon}C_1^2. \tag{21}$$

On the other hand, since the terms with the exogenous chemorepellent have opposite sign, the following lower bounds will be useful

$$\begin{aligned}\chi_r p\int_\Omega n_m^p\nabla c_r\cdot\nabla n_m d\mathbf{x} &= p\int_\Omega\frac{2}{p+1}\nabla n_m^{\frac{p+1}{2}}\cdot\chi_r n_m^{\frac{p+1}{2}}\nabla c_r d\mathbf{x}\\ &\ge -p\int_\Omega\frac{2}{p+1}|\nabla n_m^{\frac{p+1}{2}}|\chi_r n_m^{\frac{p+1}{2}}|\nabla c_r|d\mathbf{x}\,.\end{aligned} \tag{22}$$

We then obtain that

$$\begin{aligned}-\chi_r p\int_\Omega n_m^p\nabla c_r\cdot\nabla n_m d\mathbf{x} &\le p\frac{\varepsilon}{(p+1)^2}\int_\Omega|\nabla n_m^{\frac{p+1}{2}}|^2 d\mathbf{x}+\frac{p\chi_r^2}{\varepsilon}\int_\Omega n_m^{p+1}|\nabla c_r|^2 d\mathbf{x}\\ &\le p\frac{\varepsilon}{(p+1)^2}\int_\Omega|\nabla n_m^{\frac{p+1}{2}}|^2 d\mathbf{x}+\frac{p\chi_r^2}{\varepsilon}C_2^2\int_\Omega n_m^{p+1}d\mathbf{x}\,,\end{aligned} \tag{23}$$

where we used Young's inequality $ab<\frac{\varepsilon}{4}a^2+\frac{1}{\varepsilon}b^2$ the assumptions of Lemma 1 and the regularity of $c_r$.

Analogously

$$\begin{aligned}-m\chi_r p\int_\Omega n_m^{p-1}\nabla c_r\cdot\nabla n_m d\mathbf{x} &\le p\int_\Omega\frac{2}{p+1}|\nabla n_m^{\frac{p+1}{2}}|m\chi_r n_m^{\frac{p-1}{2}}|\nabla c_r|d\mathbf{x}\\ &\le p\frac{\varepsilon}{(p+1)^2}\int_\Omega|\nabla n_m^{\frac{p+1}{2}}|^2 d\mathbf{x}+\frac{p(m\chi_r)^2}{\varepsilon}C_2^2\int_\Omega n_m^{p-1}d\mathbf{x}\\ &\quad+\frac{p(m\chi_r)^2}{\varepsilon}C_2^2\int_\Omega n_m^{p+1}d\mathbf{x}+\frac{p(m\chi_r)^2}{\varepsilon}C_2^2\,,\end{aligned} \tag{24}$$

where we used the simple inequality $a^{p-1}\le a^{p+1}+1$, which is valid for every $a\ge 0$ and $p\ge 1$.

Coupling all the estimates above, one obtains

$$\begin{aligned}\frac{d}{dt}\int_\Omega n_m^{p+1}d\mathbf{x} &\le -\frac{p}{(p+1)}\int_\Omega(4f(n)-4\varepsilon)|\nabla n_m^{\frac{p+1}{2}}|^2 d\mathbf{x}\\ &\quad+p(p+1)C\int_\Omega n_m^{p+1}d\mathbf{x}+p(p+1)C\,,\end{aligned} \tag{25}$$

where $C$ is a generic constant that depends only on $\varepsilon$, $m$, $\chi$ and $\chi_r$. Except for the dependence of $C$ on $\chi_r$, this is the same results found in [14], so we can easily conclude the proof following the same steps. □

**Lemma 2.** *Let $\Omega$ be an open, bounded domain in $\mathbb{R}^2$ with $C^1$ boundary. For every $1<p<+\infty$ and $h$, such that there exists $\bar n>0$, such that*

$$f(n)=nh'(n)\ge\frac{(p+1)^2\pi}{p}C_\Omega a\chi\theta\qquad\forall\, n\ge\bar n, \tag{26}$$

*the $L^p$ norm of solution $n=n(t,\mathbf{x})$ to (13) is bounded*

$$||n(t)||_{L^p}\le C(\bar n,p,t)\quad\forall\, t<T_{max} \tag{27}$$

*where $C$ exponentially increases with $t$.*

*Proof.* To begin the proof we turn back to (19) and write

$$\frac{d}{dt}\int_\Omega n_m^{p+1}d\mathbf{x} - \frac{4p}{(p+1)}\int_\Omega f(n)|\nabla n_m^{\frac{p+1}{2}}|^2 d\mathbf{x} + \chi p(p+1)\int_\Omega (n_m^p + mn_m^{p-1})\nabla c\cdot\nabla n_m d\mathbf{x} - \chi_r p(p+1)\int_\Omega (n_m^p + mn_m^{p-1})\nabla c_r\cdot\nabla n_m d\mathbf{x}\,. \tag{28}$$

As in the proof of Lemma 2.2 in [15], it can be seen that

$$-\frac{4p}{(p+1)}\int_\Omega f(n)|\nabla n_m^{\frac{p+1}{2}}|^2 d\mathbf{x} + \chi p(p+1)\int_\Omega (n_m^p + mn_m^{p-1})\nabla c\cdot\nabla n_m d\mathbf{x} \le -\frac{2p}{p+1}\int_\Omega F(n,m,p)|\nabla n_m^{\frac{p+1}{2}}|^2 d\mathbf{x} + C_2\int_\Omega n_m^{p+1} + C_1\,, \tag{29}$$

where $C_1 = m^2 a\chi(p+1)$, $C_2 = ma\chi(2p+1) + m^2 a\chi(p+1) + 4C_\Omega\pi\theta\chi ap$, and

$$F(n,m,p) = 2f(n) - 2C_\Omega a\chi\pi\theta\frac{(p+2)^2}{p+1}.$$

The last terms of (28) can be estimated as follows:

$$\begin{aligned} -\chi_r p(p+1)\int_\Omega (n_m^p + mn_m^{p-1})\nabla c_r\cdot\nabla n_m d\mathbf{x} &= \\ &= -\chi_r p\int_\Omega \nabla n_m^{p+1}\cdot\nabla c_r d\mathbf{x} - m\chi_r(p+1)\int_\Omega \nabla n_m^p\cdot\nabla c_r d\mathbf{x} = \\ &= \chi_r p\int_\Omega n_m^{p+1}\Delta c_r d\mathbf{x} + m\chi_r(p+1)\int_\Omega n_m^p\Delta c_r d\mathbf{x} = \\ &= -\chi_r p\int_\Omega n_m^{p+1}\Sigma_r(\mathbf{x})d\mathbf{x} + \chi_r p\mu_r\int_\Omega n_m^{p+1}c_r d\mathbf{x} \\ &\quad - m\chi_r(p+1)\int_\Omega n_m^p\Sigma_r(\mathbf{x})d\mathbf{x} + \chi_r(p+1)\mu_r\int_\Omega n_m^p c_r d\mathbf{x}\,, \end{aligned} \tag{30}$$

where $\Sigma_r(\mathbf{x}) = \frac{H_r(\mathbf{x})}{D_r}$. Since this function is a source term, it is assumed non-negative, and then

$$-\chi_r p(p+1)\int_\Omega (n_m^p + mn_m^{p-1})\nabla c_r\cdot\nabla n_m d\mathbf{x} \le \chi_r p\mu_r\int_\Omega n_m^{p+1}c_r d\mathbf{x} + \chi_r(p+1)\mu_r\int_\Omega n_m^p c_r d\mathbf{x}\,. \tag{31}$$

From the properties of $c_r$, that is $c_r \in W^{2,\infty}(\Omega)\cap H^3(\Omega)$, it follows that $||c_r||_{L^\infty} \le \bar{C}$ and so

$$\chi_r p\mu_r\int_\Omega n_m^{p+1}c_r d\mathbf{x} \le \chi_r p\mu_r\bar{C}\int_\Omega n_m^{p+1}d\mathbf{x} \tag{32}$$

$$\chi_r(p+1)\mu_r\int_\Omega n_m^p c_r d\mathbf{x} \le \chi_r(p+1)\mu_r\bar{C}\int_\Omega n_m^p d\mathbf{x} \le \chi_r(p+1)\mu_r\bar{C}\int_\Omega n_m^{p+1}d\mathbf{x} + m\chi_r(p+1)\mu_r\bar{C}, \tag{33}$$

recalling that $n_m^p \le n_m^{p+1} + 1$.

Coupling (29) with (32) and (33), and taking into account that from the assumptions of Lemma 2 $F(n,m,p) \geq 0$ for any $n \geq m$ (once assumed $m \geq \bar{n}$), we can write

$$\begin{aligned}\frac{d}{dt}\int_\Omega n_m^{p+1}d\mathbf{x} \leq C_2\int_\Omega n_m^{p+1} + C_1 + \chi_r p\mu_r\bar{C}\int_\Omega n_m^{p+1}d\mathbf{x} + \chi_r(p+1)\mu_r\bar{C}\int_\Omega n_m^{p+1}d\mathbf{x} \\ + m\chi_r(p+1)\mu_r\bar{C} \\ = \bar{C}_2\int_\Omega n_m^{p+1}d\mathbf{x} + \bar{C}_1\,,\end{aligned} \tag{34}$$

where $\bar{C}_1 = C_1 + m\chi_r(p+1)\mu_r\bar{C}$ and $\bar{C}_2 = C_2 + \chi_r p\mu_r\bar{C} + m\chi_r(p+1)\mu_r\bar{C}$.

Taking $m \geq ||n_0||_{L^\infty}$ it follows that

$$\int_\Omega n_m^{p+1}d\mathbf{x} \leq \frac{\bar{C}_1}{\bar{C}_2}\left(\mathrm{e}^{\bar{C}_2 t} - 1\right) \qquad \forall\, t > 0 \tag{35}$$

which leads to the thesis of Lemma 2. □

The following theorem gives a sufficient condition for the a priori boundedness of solutions to (13) at any not necessarily finite time.

**Theorem 2.** *Let $\Omega$ be an open, bounded domain in $\mathbb{R}^2$ with $C^{1,1}$ boundary. Assume that there exists $\varepsilon > 0$ and $\bar{n} > 0$, such that $nh'(n) \geq \varepsilon$ for all $n \geq \bar{n}$. Moreover, assume that there exists a function $W(n)$, such that*

$$W''(n) = \frac{f(n)}{n} \tag{36}$$

*and*

$$W(n) > \eta n^p \tag{37}$$

*for some $p > 2$, $\eta > 0$ and every $n \geq \bar{n}$. Then for every finite $T$ the solution to (13) is uniformly bounded in $[0,T]$, where the estimate does not depend on $T$. Moreover, $\exists\ 0 < M < +\infty : \forall\, t < T_{max} \leq +\infty,\ ||n(t)||_{L^\infty} \leq M$.*

*Proof.* We introduce a Lyapunov function for our Problem (13), that has the following form

$$\begin{aligned}H(n,c,c_r) =& \frac{1}{2}\int_\Omega |\nabla c|^2 d\mathbf{x} + \frac{\mu}{2}\int_\Omega c^2 d\mathbf{x} + \frac{a}{\chi}\int_\Omega W(n)d\mathbf{x} \\ & - a\int_\Omega ncd\mathbf{x} + a\int_\Omega \frac{\chi_r}{\chi}nc_r d\mathbf{x},\end{aligned} \tag{38}$$

where $W$ is as in Theorem 2 and $\Sigma_r(\mathbf{x}) = D_r^{-1}H_r(\mathbf{x})$. One then has

$$\begin{aligned}\frac{dH(n,c,c_r)}{dt} =& \int_\Omega \nabla c\cdot\nabla\left(\frac{\partial c}{\partial t}\right)d\mathbf{x} + \mu\int_\Omega c\frac{\partial c}{\partial t}d\mathbf{x} + \frac{a}{\chi}\int_\Omega W'(n)\frac{\partial n}{\partial t}d\mathbf{x} \\ & - a\int_\Omega n\frac{\partial c}{\partial t}d\mathbf{x} - a\int_\Omega c\frac{\partial n}{\partial t}d\mathbf{x} + a\frac{\chi_r}{\chi}\int_\Omega n\frac{\partial c_r}{\partial t}d\mathbf{x} + a\frac{\chi_r}{\chi}\int_\Omega c_r\frac{\partial n}{\partial t}d\mathbf{x}\end{aligned} \tag{39}$$

Using Green's theorem and zero Neumann boundary conditions, and applying the equations (13), one obtains

$$\frac{dH(n,c,c_r)}{dt} = a\int_\Omega\left(\frac{1}{\chi}W'(n) - c + \frac{\chi_r}{\chi}c_r\right)\nabla\cdot(f(n)\nabla n - \chi n\nabla c + \chi_r n\nabla c_r)d\mathbf{x} \tag{40}$$

Using again Green's theorem one gets

$$\frac{dH(n,c,c_r)}{dt} = -\frac{a}{\chi}\int_\Omega (W''(n)\nabla n - \chi\nabla c + \chi_r\nabla c_r)\cdot(f(n)\nabla n - \chi n\nabla c + \chi_r n\nabla c_r)d\mathbf{x}. \tag{41}$$

Applying the assumption (36) one obtains

$$\frac{dH(n,c,c_r)}{dt} = -\frac{a}{\chi}\int_\Omega \frac{1}{n}\left|f(n)\nabla n - \chi n\nabla c + \chi_r n\nabla c_r\right|^2 d\mathbf{x} \le 0. \tag{42}$$

This means that $H(n,c,c_r) \le H(n_0,c_0,c_r)$ for every $t>0$, where $c_0$ and $c_r$ are solutions of the elliptic equations

$$\begin{cases} -\Delta c + \mu c = a n_0 & \text{in} \quad \Omega \\ -\Delta c_r + \mu_r c_r = \Sigma_r(\mathbf{x}) & \text{in} \quad \Omega \\ \nabla c\cdot\mathbf{N} = \nabla c_r\cdot\mathbf{N} = 0 & \text{on} \quad \partial\Omega \end{cases} \tag{43}$$

We have also to prove that the function $H(n,c,c_r)$ is bounded from below. To check it we apply Young's inequality

$$-\int_\Omega ncd\mathbf{x} \ge -\frac{1}{2\varepsilon}\int_\Omega n^2 d\mathbf{x} - \frac{\varepsilon}{2}\int_\Omega c^2 d\mathbf{x}$$

in equation (38). We obtain

$$\begin{aligned} H(n,c,c_r) &\ge \frac{1}{2}\int_\Omega |\nabla c|^2 d\mathbf{x} + \frac{1}{2}(\mu - a\varepsilon)\int_\Omega c^2 d\mathbf{x} + \frac{a}{\chi}\int_\Omega W(n)d\mathbf{x} \\ &\quad - a\frac{1}{2\varepsilon}\int_\Omega n^2 d\mathbf{x} + a\frac{\chi_r}{\chi}\int_\Omega nc_r \\ &\ge \frac{1}{2}\int_\Omega |\nabla c|^2 d\mathbf{x} + \frac{1}{2}(\mu - a\varepsilon)\int_\Omega c^2 d\mathbf{x} + \frac{a}{\chi}\int_\Omega W(n)d\mathbf{x} - a\frac{1}{2\varepsilon}\int_\Omega n^2 d\mathbf{x}, \end{aligned} \tag{44}$$

since the last term is nonnegative. Assumption (37) allows to write that

$$W(n) \ge \frac{\chi}{2\varepsilon}n^2$$

provided that

$$n \ge \tilde{n} = \max\left\{\bar{n},\ \sqrt[p-2]{\frac{\chi}{2\varepsilon\eta}}\right\}.$$

Therefore, one gets

$$\frac{a}{\chi}\int_\Omega W(n)d\mathbf{x} - a\frac{1}{2\varepsilon}\int_\Omega n^2 d\mathbf{x} \ge -\bar{H} = \min\left\{0, \frac{a}{\chi}\min_{n\le\bar{n}}(W(n) - \frac{\chi}{2\varepsilon}n^2)\right\}. \tag{45}$$

Thus, taking $\varepsilon < \frac{\mu}{a}$, we obtain

$$H(n,c,c_r) \ge -\bar{H} \tag{46}$$

and then we get

$$H(n_0,c_0,c_r) \ge H(n,c,c_r) \ge -\bar{H}. \tag{47}$$

As in [14] it follows from inequalities (44), (46) and (47) that $c$ belongs to $H^1(\Omega)$ uniformly in time:

$$||c(t)||^2_{H^1(\Omega)} \le \frac{2(H(n_0,c_0,c_r)+\bar{H})}{\min\{1,\mu - a\varepsilon\}} \qquad \forall\, t>0.$$

Once at this point, we can follow the proof of Theorem 4.2 in [14] and easily conclude. □

**Conclusions and Remarks.** We have deduced a model with the aim of predicting the qualitative structure of the capillary network induced in the presence of exogenous chemical factors. Comparing the results obtained using chemoattractant and chemorepellent factors, it seems that the latter are more effective in controlling the shape of the structure.

We put in evidence the importance of the range of action of the chemical factors and the fact that chemoattractants induce in their range of action the formation of capillaries which depart from the source of chemoattractant, while chemorepellents induce the formation of capillaries which surround the source of chemorepellent, where its range of influence is fading away.

We are confident that the model presented here can be used to identify the optimal placement of exogenous chemical factors in the induction of vascular networks in vitro.

## REFERENCES

[1] D. Ambrosi, F. Bussolino, and L. Preziosi, *A review of vasculogenesis models*, J. Theor. Med., **6** (2005), 1–19.

[2] D. Ambrosi, A. Gamba, and G. Serini, *Cell directionality and chemotaxis in vascular morphogenesis*, Bull. Math. Biol., **66** (2004), 1851–1873.

[3] P.D. Chilibeck, D.H. Paterson, D.A. Cunningham, A.W Taylor, and E.G. Noble, *Muscle capillarization O2 diffusion distance, and VO2 kinetics in old and young individuals*, J. Appl. Physiol., **82** (1997), 63–69.

[4] A. Coniglio, A. de Candia, S. Di Talia, and A. Gamba, *Percolation and Burgers' dynamics in a model of capillary formation*, Phys. Rev. E, **69** (2004), 051910.

[5] F. Filbet, P. Laurencot, and B. Perthame, *Derivation of hyperbolic models for chemosensitive movement*, J. Math. Biol., **50** (2005), 189–207.

[6] J. Folkman and C. Haudenschild, *Angiogenesis in vitro*, Nature, **288** (1980), 551–556.

[7] P. Friedl, *Prespecification and plasticity: shifting mechanisms of cell migration*, Curr. Opin. Cell. Biol., **16** (2004), 14–23.

[8] A. Gamba, D. Ambrosi, A. Coniglio, A. de Candia, S. Di Talia, E. Giraudo, G. Serini, L. Preziosi, and F. Bussolino, *Percolation, morphogenesis and Burgers dynamics in blood vessels formation*, Phys. Rev. Lett., **90** (2003), 118101.

[9] D. Grant, K. Tashiro, B. Segui-Real, Y. Yamada, G. Martin, and H. Kleinman, *Two different laminin domains mediate the differentiation of human endothelial cells into capillary-like structures in vitro*, Cell, **58** (1989), 933–943.

[10] G.J. Goodhill, *Mathematical guidance for axons*, Trends in Neurosci., **21** (1998), 226–231.

[11] A. Guyton and J. Hall, *Textbook of Medical Physiology,* W.B. Saunders, St. Louis, 2000.

[12] T. Huynh, G. Abraham, J. Murray, K. Brockbank, P.O. Hagen, and S. Sullivan S., *Remodeling of an acellular collagen graft into a physiologically responsive neovessel*, Nature Biotech., **17** (1999), 1083–1086.

[13] S. Kaushal, G.E. Amiel, K.J. Guleserian, O.M. Shapira, T. Perry, F.W. Sutherland, E. Rabkin, A.M. Moran, F.J. Schoen, A. Atala, S. Soker, J. Bischoff, J.E. Mayer Jr., *Functional small-diameter neovessels created using endothelial progenitor cells expanded ex vivo*, Nature Med., **7** (2001), 1035–1040.

[14] R. Kowalczyk, *Preventing blow-up in a chemotaxis model*, J. Math. Anal. Appl., **305** (2005), 566-588.

[15] R. Kowalczyk, *Modelling cell aggregation in vasculogenesis*, PhD Thesis, Politecnico di Torino (2004).

[16] R. Kowalczyk, A. Gamba, and L. Preziosi, *On the stability of homogeneous solutions to some aggregation models*, Discr. Cont. Dyn. Sys. B, **4** (2004), 203–220.

[17] A. Krogh, *The number and distribution of capillaries in muscle with calculations of the oxygen pressure head necessary for supplying the tissue*, J. Physiol., **52** (1919), 409–415.

[18] Kubota, Y., Kleinman, H., Martin, G., and Lawley, T., "Role of laminin and basement membrane in the morphological differentiation of human endothelial cells into capillary-like structures", *J. Cell Biol.* **107** (1988), 1589–1598.

[19] R.M.H. Merks, S.A. Newman, and J.A. Glazier, *Dynamic mechanisms of blood vessel growth*, Nonlinearity, **19** (2006), C1–C10.
[20] R.M. Nerem and D. Seliktar, *Vascular tissue engineering*, Ann. Rev. Biomed. Engng., **3** (2001), 225–243.
[21] T. Richardson, M. Peters, A. Ennett, and D. Mooney, *Functional small-diameter neovessels created using endothelial progenitor cells expanded ex vivo*, Nature Biotech., **19** (2001), 1029–1034.
[22] G. Serini, D. Ambrosi, E. Giraudo, A. Gamba, L. Preziosi, and F. Bussolino, *Modeling the early stages of vascular network assembly*, EMBO J., **22** (2003), 1771–1779.
[23] S. Shandarin and Y. Zeldovich, *The large-scale structure of the universe: Turbulence, intermittency, structures in a self-gravitating medium*, Rev. Mod. Phys., **61** (1989), 185–220.
[24] A. Tosin, D. Ambrosi, and L. Preziosi, *Mechanics and chemotaxis in the morphogenesis of vascular networks*, Bull. Math. Biol., **68** (2006).
[25] B. Vailhé, D. Vittet, and J.J. Feige, *In vitro models of vasculogenesis and angiogenesis*, Lab. Investig., **81** (2001), 439–452.
[26] M. Vergassola, B. Dubrulle, U. Frisch, and A. Noullez, *Burgers' equation, devil's staircases and the mass distribution for large-scale structures*, Astron. Astrophys., **289** (1994), 325–356.
[27] D.J. Webb and A.F. Horwitz, *New dimensions in cell migration*, Nature Cell Biol., **5** (2003), 690–692.
[28] K. Wolf, I. Mazo, H. Leung, K. Engelke, U.H. von Andrian, E.I. Deryugina, A.Y. Strongin, E.-B. Bröcker, and P. Friedl, *Compensation mechanism in tumor cell migration: mesenchimal–ameboid transition after blocking of pericellular proteolysis*, J. Cell. Biol., **160** (2003), 267–277.

Received July 2006; revised September 2006.

*E-mail address*: luigi.preziosi@polito.it